Introduction

Schizophrenia spectrum and other psychotic disorders (SSD) affect up to 3% of the population [1], are accompanied by prominent social and occupational functional impairments, and represent one of the leading causes of disability worldwide [2]. Symptoms associated with SSD comprise the following key dimensions: positive symptoms (e.g., hallucinations, delusions), negative symptoms (e.g., blunted affect, avolition), disorganized thinking (e.g., derailment, loose associations), abnormal motor behavior (e.g., catatonia) and cognitive deficits (e.g., memory impairments), as well as affective symptoms (e.g., mania, anxiety, depression) [3, 4]. SSD can be studied along a developmental continuum, ranging from clinical-high risk (CHR), with sub-threshold psychotic symptoms and increased risk of developing a first-episode of psychosis (FEP), to enduring schizophrenia [5]. This clinical staging model provides a framework to study the neurobiological correlates related to the potential risk, onset, and progression of SSD [6].

Magnetic resonance imaging (MRI), through its various modalities, has tentatively characterized such correlates and continues providing new insights into the pathophysiology of these disorders [7, 8]. Notably, Blood-oxygen-level-dependent imaging (BOLD-MRI) studies have demonstrated modified brain activation over the course of illness and in relation to positive and negative symptomatology [9, 10]. However, the BOLD signal (i.e., local change in oxyhemoglobin/deoxyhemoglobin) has a complex relationship with functional brain activity, oxidative metabolism, and neurovascular factors rendering it difficult to interpret [11]. The BOLD signal is accompanied by an increase in blood flow, blood volume, and oxygen consumption, thought to reflect local changes in neural activity. Given the complex and ambiguous nature of the BOLD signal, the exploration of cerebral blood flow (CBF) itself could shed light on specific hemodynamic pathological correlates. CBF is the measure of the volume of blood per unit time (ml/min), and is typically measured as perfusion in a given quantity of brain tissue (ml/100g tissue/min) [12]. The exploration of CBF can be global or regional, at rest or in response to vasoactive stimulation (e.g., hypercapnia manipulation, cognitive or behavioral tasks). CBF and its regulation through cerebrovascular reactivity (CVR, the hemodynamic response to a global vasoactive stimulus such as CO2) and neurovascular coupling (NVC) are thought to reflect the brain's metabolism and its attempt to meet the metabolic demands of neural activity [13]. This coupling between metabolism, neural activity and blood flow is thought to be achieved via the neurovascular unit (NVU) which embody the unique relationship between brain cells (e.g., neurons, glia) and the vascular system (e.g., endothelium, pericytes) [14]. The main function of this coupling is to maintain homeostasis by delivering the energy substrates (e.g., O2, glucose) needed to initiate and sustain neural activity, while clearing potentially toxic by-products of brain metabolism (e.g., CO2, lactate, heat) [14]. This involves a coordinated multi-dimensional response that might

be altered at different levels and evidenced by abnormal CBF, CVR or NVC. In a reversal of roles, hemodynamic factors could also influence the neural activity via mechanical, thermal, or chemical effects on the NVU (i.e., vasculo-neuronal coupling) [15, 16]. Finally, there is a strong body of evidence suggesting that structural and functional alterations of the NVU are associated with various neurodegenerative disorders [14], as well as mental disorders, such as autism spectrum disorder, anxiety, depression and schizophrenia [17, 18].

Since CBF was first quantified in humans by Kety and Schmidt [19], techniques used to measure brain perfusion have evolved from direct blood sampling to functional nuclear imaging, such as single-photon emission computed tomography (SPECT), positron emission tomography (PET) and most recently perfusion MRI. While PET and SPECT provided many of the findings that are key to our contemporary understanding of brain perfusion, they are limited by their reliance on radioisotopes and consequent radiation exposure. The two most common perfusion MRI methods are dynamic susceptibility contrast (DSC) and arterial spin labeling (ASL, the basic principles, advantages, and disadvantages of which are summarized in Table 1). ASL relies upon a relatively simple modification to a standard gradient echo MRI acquisition analogous to that used for BOLD: before the acquisition of the brain image, blood in the neck is converted into an endogenous MR tracer by the process of magnetic inversion of the hydrogen nuclei (i.e., spin) in water, commonly called labeling. After a delay period, which allows for blood to flow into the brain, where it accumulates within the tissue by crossing from the blood into cells and the extracellular space, the image acquired. The image thus contains information about the delivery of the tracer to the tissue. By comparing it with a control image, in which no labeling has been done, an image of perfusion can be obtained. Hence, the basic ASL experiment contains a pair of images: label and control. A typical acquisition collects multiple pairs of images to improve the signal-to-noise ratio. The labeling schemes and their variations in the timing and the plane of the radiofrequency fields applied are responsible for a variety of acquisition methods in ASL of which most recent technical development have been recently reviewed by Hernandez-Garcia et al., (2022) [20]. With continuous (cASL) and pseudo-continuous (pCASL) ASL, any blood flowing through a defined labeling plane at the level of the carotids is inverted whereas with pulsed ASL (pASL), a single brief labeling pulse inverts all the blood-water spins within some spatial region [12]. ASL imaging has been validated extensively against other perfusion methods by demonstrating accurate and reproducible quantification of CBF [21-24]. Since it is completely non-invasive, ASL imaging has become useful for many clinical and research applications [25-28].

In psychosis, abnormal distribution of regional CBF (rCBF) was originally shown in PET/SPECT studies [29]. Notably, the hypofrontality concept emerged from this technique and was initially suggested

in the mid-70s by Ingvar, Franzén [30]. Their seminal paper described reduced perfusion in the frontal area of 31 patients with chronic schizophrenia, due to a gradient of frontal to posterior blood flow. Since then, this concept has gained significant support and been repeatedly described through various modalities [31, 32]. In the first meta-analysis conducted by Hill et al., (2004) conflicting findings regarding resting hypofrontality led to the suggestion that this alteration was progressive and related to the chronicity of psychotic episodes [31]. The temporal area has also been a region of interest with the observation of a reduced left to right hemisphere gradient of cerebral blood flow in this region [33]. More recently Guimarães et al., (2016) reviewed ASL studies in enduring schizophrenia and retrieved CBF findings from ten studies [34]. They identified predominantly decreased rCBF across the brain except in the putamen, which they interpreted as related to potential clinical and cognitive impairments [34]. Hypoperfusion was mainly observed in the frontal area, notably in the middle and inferior frontal gyri, anterior cingulate cortex, and to a lesser extent in the occipito-temporal regions, and parietal area. rCBF results pertaining to the middle temporal gyrus and the thalamus, for their part, were more equivocal [34]. While these initial ASL results supported previous PET/SPECT findings, generalizability is limited as six out of the ten studies included were conducted on a small sample ($n < 20$), totaling only 297 schizophrenia patients that could not allow the exploration of correlates of symptoms dimensions nor any other clinical stages. This confirms the necessity of further exploring rCBF in SSD populations with larger samples, in relation to symptomatology and progression of psychosis.

Since this review dating from 2016, ASL has become increasingly accessible and has gained in popularity, with more than 400 new publications per year in all fields combined reported on PubMed® in the last 5 years. This includes the publication of consensus recommendations from the Perfusion Study Group of the International Society for Magnetic Resonance in Medicine [35]. To our knowledge, there is no recent review of this literature nor any comprehensive meta-analysis of perfusion MRI findings in SSD. Given the expansion of a well-suited method to explore perfusion in clinical populations, we first sought to conduct an updated systematic review of MRI-based perfusion studies exploring CBF across the different clinical stages of SSD. Our goals were: 1) to qualify rCBF differences between enduring SSD patients and healthy individuals, 2) to examine the relationship between rCBF and psychotic symptoms, and 3) to assess stage-specific perfusion correlates. Second, we conducted a meta-analysis on whole-brain studies to quantify resting-state rCBF differences between enduring SSD patients and healthy individuals.

Methods

Registration, Databases and Search terms

This systematic literature review followed a registered protocol (PROSPERO: CRD42020197538) and reporting was done in accordance with the Preferred Reporting Items for Systematic Reviews and Meta-analyses statement [36]. MRI-based perfusion studies in SSD were identified from peer-reviewed human research articles published in English. A systematic OVID search was performed in Embase, MEDLINEOvid, and PsycINFO using the following terms: **1)** schizophreni* OR psychosis OR psychoses OR psychot* OR "schizo af*" AND; **2)** "magnetic resonance imaging" OR MRI OR fMRI OR "arterial spin label*" OR ASL OR "resting state" OR "perfusion weighted imaging" OR PWI AND; **3)** Perfusion OR "cerebral blood flow" OR CBF OR "cerebrovascular reactivity" OR CVR OR "cerebral vascular reactivity" OR "cerebrovascular reactivity" OR "cerebral vasoreactivity" OR "cerebral vasomotor reactivity" OR "vasomotor responsiveness" OR "cerebrovascular responsiveness". Terms were searched in the following fields: title, abstract or keywords. No time span was specified for the database queries (initial search: September 2020; updated search: August 2022). Additional records were sought from the reference sections of included papers and perfusion neuroimaging reviews in psychiatric disorders.

Inclusion and exclusion criteria

After removal of duplicates, the titles and abstracts of all retrieved articles were independently screened by two of the authors (O.P., D.R-C). The two reviewers had a substantial agreement (Kappa statistic (κ) = 0.851). Disagreements between the reviewers were discussed and resolved during consensus meetings. Studies eligible for inclusion in the systematic review met the following criteria: **1)** involved individuals with clinical- or ultra-high risk for psychosis, first-episode psychosis or schizophrenia spectrum and other non-affective psychotic disorders **2)** along with healthy controls; **3)** MRI-based perfusion imaging methods were used (e.g., ASL, DSC); **4)** CBF and/or CVR findings were reported. Exclusion criteria were: **1)** affective psychotic disorders (e.g., bipolar disorder or major depressive disorder with psychotic features); **2)** non-MRI-based perfusion imaging (e.g., single-photon emission computed tomography, positron emission tomography); **3)** conference abstracts, case reports, reviews and meta-analyses. Full texts of the remaining articles were assessed for eligibility and a final decision was made regarding inclusion. Studies were further included in a meta-analysis, if: **1)** whole-brain analyses of **2)** resting-state and **3)** regional CBF were conducted **4)** between a complete sample of enduring SSD patients and HC. In case of overlap between studies sample, defined as 50% of participants in common, only the study with the highest quality score remained included in the meta-analysis.

Risk of Bias Assessment

To assess the methodological quality of included studies, the risk of bias was calculated according to an adapted version of the quality analysis tool for ASL studies recently published by Sukumar et al., (2020) [37] and further detailed in Supplementary Table S1. Fifteen items were examined, according to four criteria dimensions: **1)** participant selection; **2)** image acquisition; **3)** image preprocessing and analysis; and **4)** statistical analysis techniques. Each criterion was rated as "adequate" (score = 1) if all aspects of the criterion were reported and met minimum standard, "inadequate" (score = 0) if aspects of the criterion were missing or did not meet minimum standard, or "intermediate" (score = 0.5) if aspects of the criterion were only partly reported (e.g., information only provided for sex, but not for age). An average score was then computed for each study with a maximum of 1. For studies using perfusion imaging method other than ASL, criteria **2)** and **3)** were adapted according to the specific recommended guidelines for that technique [38].

Data Extraction

Three researchers (O.P., D.R-C, J.U.) independently extracted the data of included studies into a Microsoft Excel spreadsheet. The spreadsheet was tested and revised prior to completing the data extraction process. Extracted variables included the following information: study authors, year of publication, study design, sample selection, sample characteristics, intervention and/or exposure description, control condition, details of the assessment, primary and secondary outcomes and measurement tools, MRI methods with MRI sequences and acquisition parameters, MRI analyses, statistical methods, and main results, attrition rate, amount of missing data. Recruitment location and period were also extracted to help identify potential overlap between study samples. For the purpose of conducting a quantitative meta-analysis, MNI/Talairach coordinates of significant peaks were extracted, as well as the covariates and significance thresholds. If data were missing, the authors were contacted by email to provide the required information. Quality control was conducted by D.R-C who checked the data extraction for completion and accuracy. Any discrepancy was resolved through consensus.

Seed-based d Mapping (SDM) meta-analysis

Studies conducting whole-brain analysis of resting-state rCBF between enduring SSD patients and HC were further meta-analyzed to quantify voxel-wise differences. Seed-based d Mapping (SDM) via permutation of subject images (PSI) was performed with SDM-PSI software version 6.21 for Linux (https://www.sdmproject.com/). Unlike other coordinate-based meta-analytic methods, which rely on

tests of spatial convergence, SDM-PSI uses a novel algorithm (PSI) validated in Albajes-Eizagirre et al., (2019) to conduct standard voxel-wise tests [39]. This allows SDM-PSI to overcome two limitations intrinsic to previous methods (i.e., that voxels are independent and have the same probability to have a "false" peak), while increasing statistical power in the presence of divergent effects [39]. The analysis was performed following the step-by-step protocol described by Albajes-Eizagirre et al., (2019) [39]. The preprocessing and main analysis were performed using the default parameters associated with the voxel-based morphometry for the grey matter modality (full anisotropy, grey matter mask, FWHM = 20 mm). Following recommendations [40], an uncorrected threshold of p = 0.005 with a cluster extent of 10 voxels and SDM- Z > 1 was applied as it is thought to adequately control the probability of detecting an effect by chance. In addition, a threshold free cluster enhancement threshold (TFCE) corrected for FWE (p = .025) was applied in a pair of one-tailed tests. The robustness of the results was assessed by conducting a jack-knife analysis. This was done by repeating the meta-analysis iteratively with a leave-one-out strategy for each included study. Each significant cluster was then given a score corresponding to the number of times it was reported among all iterations. Finally, we analyzed the residual heterogeneity, and each cluster was tested for small-study effect (i.e., whether larger effect sizes are observed in smaller studies) as well as a for excess significance (i.e., whether the number of significant findings is larger than expected) using the Bias Analysis option of SDM-PSI [39]. Funnel plots of effect sizes for each cluster were visually inspected for asymmetries.

Results

Search results and general descriptions of reviewed studies

The Ovid search yielded 648 publications. Following the removal of duplicates and conference abstracts, 146 publications remained. The screening of titles and abstracts by O.P. and D.R-C yielded 65 articles to undergo full-text assessment for eligibility. Twenty-four additional articles were further excluded as they did not meet one or more of the selection criteria. One additional article was identified through reference list search [41]. Thus, 42 articles comprising 1872 patients and 1608 controls were included in the systematic review of which 17 studies could be meta-analyzed. Figure 1 illustrates the PRISMA flowchart and Table 2 presents the general characteristics of the reviewed studies.

Overall, 41 studies explored resting-state CBF and one examined CVR using a hypercapnia challenge [41]. Only three of them investigated NVC with a cognitive task [41, 42] or an emotion processing task [43]. Among CBF studies, 4 used DSC and 37 ASL methods. More precisely, pCASL was performed in 28 studies (published between 2013 and 2022), PASL in eight studies (published between 2009 and 2021),

and CASL in one study (published in 2010). The risk of bias was assessed for each study and reported in Supplementary Figure S1. Studies with a score above the 25th upper percentile (score > 0.75) were considered as reflecting a low risk of bias and were prioritized when interpreting results. Concerning the continuum of populations examined, only 4 studies examined FEP patients (n=216) [44-47] and 3 studies examined CHR individuals (n=226) [48-50]. Enduring SSD patients (n=1430) were examined in the remaining 35 studies, either including schizophrenia patients only (n=23) or combining ICD/DSM diagnoses of schizophrenia and schizoaffective disorder (n=12). Overall, 12 studies split the clinical sample according to various variables of interest (i.e., symptomatology, gender, age).

Detailed analysis of reviewed studies

Group differences between enduring SSD patients and healthy controls

Out of the 35 studies exploring perfusion in enduring SSD patients, 20 reported significant rCBF differences with HC, 7 reported significant rCBF differences between subgroups of patients and 1 reported significant CVR differences. In total, 8 studies did not find any significant differences. For each cluster, we determined the broader area of the brain of which it was situated (e,g., frontal lobe, cerebellum, etc). We observed 29 clusters in frontal lobe, 18 in temporal lobe, 8 in parietal lobe, and 12 in occipital lobe. We also identified 8 clusters in limbic area, 25 in subcortical areas, 3 in cerebellum, and 3 in corpus callosum. Seven other clusters overlapped with different regions. In the frontal area, the vast majority of results (25 out of 29) revealed hypoperfusion in the SSD group relative to HC, notably in the middle frontal gyrus (MFG; 8 clusters). Similar results were observed for the temporal area, with 13 out of 18 clusters displaying lower rCBF in the SSD group, especially in the middle temporal gyrus (MTG; 4 clusters) and insula (3 clusters). Hypoperfusion in the SSD group was also shown in the parietal area (6 out of 8), the occipital area (11 out of 12) including the middle occipital gyrus (MOG; 5 clusters), the limbic area (6 out of 7), mostly in the anterior cingulate cortex (ACC; 4 clusters), the cerebellum (3 out of 3), and the corpus callosum (3 out of 3). On the contrary, in the subcortical region, unlike the other brain regions, SSD groups displayed hyperperfusion when compared to HC in 22 out of 25 clusters, notably in the putamen (8 clusters) and the thalamus (4 clusters). The only study exploring CVR reported an increased reactivity in schizophrenia when compared to HC during a breath-hold task [41]. All results are reported in Supplementary Table and Figure S2 with the terminology used in the original publication and are presented according to the region, the direction of the group contrast, the brain lateralization, the labeled name of the cluster, and the cluster size.

Relationships between cerebral blood flow and symptomatology

Clinical symptoms were explored in two ways. First, several studies conducted correlational analyses between rCBF and clinical scores. Twelve studies revealed significant correlations. The main clinical dimensions explored were: general psychopathology (one cluster), positive symptoms (10 clusters), negative symptoms (10 clusters), disorganization (6 clusters), catatonia (6 clusters), insight (3 clusters) and antipsychotic dosage (10 clusters). Results presented in Supplementary Table S3 were organized according to the clinical dimension, the direction of the correlation, the region of the cluster, the lateralization, and the labeled name of the cluster. For positive symptoms, we mainly observed positive correlations with the different brain areas (8 clusters) and two negative correlations with the precentral gyrus and frontal white matter [51], whereas negative symptoms were mainly negatively correlated to brain perfusion (6 clusters), except for two positive correlations in the temporal area [52] and two in the striatum [53] (Figure 3). Additional results are presented in Supplementary Table S4.

Group differences between early stages patients and healthy controls

Out of the seven studies exploring early stages psychosis, three did not report any significant result when contrasting with controls [44, 46, 50]. As in the SSD population, first-episode drug-naïve schizophrenia patients showed decreased rCBF in occipital and temporal regions as well as increased rCBF in subcortical regions [47]. In contrast, CHR individuals presented widespread hyperperfusions across frontal (6 clusters), temporal (4 clusters), occipital (3 clusters) and subcortical (4 clusters) regions. Supplementary Table S4 reports all significant results.

Meta-analysis results

Overall, thirteen studies conducting whole-brain analyses of resting state rCBF across 426 SSD patients and 401 HC were included in the quantitative review (written in bold in Table 2), 11 of which reported significant differences when compared to HC. Applying an uncorrected threshold (p = 0.005), clusters of hypoperfusion were identified in the left superior and middle frontal gyri (94 [21, 174] voxels, z = -3.02 [-3.25, -2.82] and 84 [30, 330] voxels, z = -3.08 [-3.82, -2.93]) along with the middle occipital gyrus (29 [14, 53] voxels, z = -3.08 [-3.3, -2.98]). In addition, hypoperfusion was also observed in the left superior temporal gyrus, left middle occipital gyrus, right superior occipital gyrus, left supramarginal gyrus, and left anterior cingulate / paracingulate gyri. However, these results failed to be significant in more than 15% of all iterations of the meta-analysis and therefore will not further be discussed as we wished to only report on the most robust results. Only one cluster of hyperperfusion was observed in the left putamen of the

lenticular nucleus (74 [44, 161] voxels, z = 3.37 [3.13, 3.77]). Neither of the hypoperfusion or hyperperfusion clusters survived the TFCE correction for FWE. All significant clusters are displayed in Table 3 and Figure 2. The low I^2 statistic (<12.4%) indicates small heterogeneity and the funnel plots does not show significant asymmetries (Supplementary Figure S3). In addition, the tests for small-study effect and excess significance did not indicate the presence of any biases (all p > 0.253).

Discussion

This updated systematic review of CBF literature in SSD was conducted with 42 MRI-based perfusion studies, extending the last published review of ASL studies in schizophrenia [34] by 32 articles. Our results revealed distinct patterns of regional cortical hypoperfusion and subcortical hyperperfusion when compared to HC. Interestingly, regional hypo- and hyperperfusions seemed associated with negative and positive symptoms respectively. Studies exploring CBF in the first stages of the SSD continuum were few. The meta-analysis of whole-brain CBF studies yielded converging results with previous reviews across different neuroimaging modalities. Hypoperfusion was notably located in fronto-occipital regions, including the SFG, MFG and MOG. In contrast, hyperperfusion was observed in the putamen.

Cortical hypoperfusion

MRI-based perfusion studies provided further support to the concept of hypofrontality as a putative pathophysiological model in SSD. As was Initially reported with SPECT/PET neuroimaging[30, 33], hypoperfusion was again observed in the frontal area, corroborating Guimaraes et al., (2016) review [34] as well as Hill et al., (2004) meta-analysis [31]. While the latter only reported overall hypofrontality, our meta-analysis improved brain localization of perfusion alterations in SSD by demonstrating decreased rCBF in the SFG and MFG. Our results also revealed significant occipital hypoperfusion in the MOG, contradicting the initial suggestion that hypoperfusion was distributed along a gradient of reduced CBF from frontal to occipital regions [30]. Our findings are in line with the bimodal meta-analysis (i.e., ASL/PET) conducted by Sukumar et al., (2020) who also reported reduced neuronal activity in fronto-occipital regions, while adding that rCBF changes were consistently associated with metabolic changes [37]. In a recent meta-analysis, the structural integrity of the SFG and MFG have been shown to drive the association between their respective functional network (i.e., the fronto-parietal and attention networks) and critically impaired cognitive domains in schizophrenia, including verbal and working memory along with reasoning and executive functions [54]. Similarly, the MOG was found to be responsible for the association between the visual network and impairments in social cognition [54]. Given their putative role in neurocognition and

social cognition, it is possible that hypoperfusion and neurovascular coupling disrupting fronto-occipital networks may be related to clinical symptoms in SSD. Reduced functional connectivity has also been observed in the visual networks [55] and our result in the MOG is in line with the recent models suggesting that visual processing is impaired in schizophrenia [56]; alterations of the neural correlates of perceptual processing could be a precursor of different cognitive and clinical impairments observed in SSD patients [57-59]. For example, besides being a precursor of visual hallucinations, Pelletier-Baldelli & Holt (2019) proposed an integrated model supporting that difficulty in filtering perceptual information associated with cognitive changes may contribute to changes in social cognition and negative symptoms.

Negative symptoms seemed negatively correlated with rCBF in fronto-limbic regions (i.e., MFG, IFG and ACC), while mixed findings were reported in temporal regions. Although such associations would need to be confirmed in a meta-regression, our results are consistent with previous structural neuroimaging studies. A decrease in grey matter volume of fronto-limbic and temporal regions has been consistently associated with negative symptoms [60-64], and this hypotrophy could relate to the observed decrease in regional perfusion. Indeed, a conjoint reduction in rCBF and grey matter volume in the ACC and insula has already been reported although the direction of the causality is open to interpretation. However, rCBF changes remained significant despite volume correction suggesting that perfusion alteration may not be caused by structural alteration [65]. Similarly, a decrease in grey matter volume in the same regions was inconsistently associated to hypoactivation or hyperactivation in previous multimodal meta-analysis [8, 66] suggesting that incongruence between neuroimaging modalities could represent normalisation, overcompensation or continued abnormality.

Furthermore, it worth noting the substantial overlap between the fronto-limbic and temporal regions identified in this review and the neural correlates found to be associated with cognitive impairments [67, 68], especially deficits in verbal, working memory, and social cognition [54]. While this observation is consistent with the robust relationship existing between negative symptoms and cognition [69-71], negative symptoms have also been shown to mediate the influence of neurocognition and social cognition on functional outcome [72-74]. Interestingly, increased baseline rCBF in the MFG predicted poor functional outcome at follow-up [75]. In this context, our results also substantiate Wojtalik et al., (2017) meta-analytic review indicating that integrity of fronto-limbic regions is consistently related to functional outcome in individuals with schizophrenia [76]. While the interplay between such dimensions can be hard to disentangle, perfusion neuroimaging offers a promising avenue to explore such relationships and perhaps identify specific hemodynamic correlates to target through intervention.

Subcortical hyperperfusion

Our review revealed regional hyperperfusions in individuals with SSD that were predominantly observed in the subcortical area, notably in the putamen. As this finding did not survive correction in our meta-analysis, it is possible that putamen metrics are associated to greater variability among patients such as already demonstrated in structural imaging [77]. Nevertheless, it contrasts Hill et al., (2004) meta-analysis as they did not report any hyperperfusion [31], while the putamen was the only region with increased rCBF in Guimaraes et al., (2016) review [34]. Interestingly, the putamen was also pointed out by Sukumar et al., (2020) who demonstrated conjoint perfusion and metabolic increase in schizophrenia [37]. Our findings are in line with the dopaminergic hypothesis of schizophrenia, in which basal ganglia and particularly striatal dopaminergic dysfunction is thought to underlie the development of psychotic symptoms [78-80]. It is possible that inconsistencies seen in the perfusion of basal ganglia may reflect the status (i.e., acute vs residual) or severity of symptoms.

Consistently, positive symptoms were positively correlated with rCBF in subcortical regions such as the lenticular nucleus (i.e., pallidum and putamen), caudate and striatum along with the hippocampus. In functional neuroimaging studies, increased activation of the putamen which contains rich dopaminergic neurons [81] has been similarly associated with hallucinations [82] and delusions [83]. Although the coupling between modalities remains to be further explored, it is possible that an increased activity, volume and/or metabolism in the putamen may result in the increased perfusion related to positive symptoms. Alternatively, rCBF alterations might be underpinned by antipsychotic action as longitudinal studies of the effects of medication have consistently shown increase in basal ganglia perfusion following treatment, particularly in the caudate [84]. Interestingly, reduction of positive symptoms has been associated with a greater increase in striatal rCBF following antipsychotic treatment [85]. Conversely, non-response to clozapine was associated with lower basal ganglia perfusion [86]. Although in this review, Zhu et al., (2015) reported a positive association in the putamen [52] with antipsychotic dosage, while the only study of antipsychotic-free SSD patients also demonstrated increased rCBF in the subcortical area [87].

In this review, we also sought to have a broader understanding of the CBF alterations found across the early stages of the illness. Although CHR and FEP studies were scarce, fronto-occipital hypoperfusions revealed in SSD are in line with decreased grey matter volume highlighted across all stages of the spectrum [88]. In addition, both initial and replication studies by Allen et al., (2016, 2018) displayed subcortical hyperperfusion in the hippocampus and pallidum/putamen in CHR [48, 49], while similar findings were reported by Chen et al., (2022) in the caudate and putamen in FEP [47]. Interestingly, improvement in positive symptoms in antipsychotic-naive patients was associated with reduced rCBF in the ventral

striatum at follow-up. Even more interestingly, only patients who no longer met CHR criteria at follow-up displayed a longitudinal reduction of rCBF in the left hippocampus. Conversely, increased rCBF in the right hippocampus at baseline predicted poor functional outcome at follow up in association with an elevated striatal dopamine synthesis capacity [50]. The resolution of the high-risk state and positive symptoms associated to the normalization of the perfusion in subcortical regions is consistent with findings from FEP and SSD populations and constitutes a compelling argument suggesting that subcortical hyperperfusion might be an early marker of SSD. However, further longitudinal research on CHR and FEP is necessary to explore the hemodynamic correlates of the transition to psychosis and confirm this subcortical pattern.

Potential perfusion markers of SSD

The cortico-subcortical contrasted pattern observed in SSD linked to the symptomatology could constitute a marker of the disorder and reflect altered perfusion covariance. Only few studies have explored CBF connectivity and, among our selection, the four that displayed CBF connectivity results used different methodologies (i.e., seed-based, independent component analysis and/or graph theory) [45, 52, 89, 90]. All studies demonstrated decreased connectivity in SSD when compared to controls. More specifically, Oliveira et al., (2018) explored the connectivity within 6 pre-identified cortical networks and reported reduced connectivity in SSD between the fronto-parietal and attention networks, substantiating our hypoperfusion results [90]. The other low risk-of-bias study revealed decreased covariance between the left thalamus (seed) and the medial part of the superior frontal gyrus (SFG) supporting functional connectivity studies [52]. Dysconnectivity between a subcortical structure and a frontal region might partially explain our contrasting results in these regions. Indeed, aberrant functional integration between cortical and subcortical structures has been highlighted with other neuroimaging modalities [7, 91] and the interdependence and strength in the coupling between brain cells and cerebral blood vessels might play a key role in the development and maintenance of SSD. Anatomical alterations of the NVU could contribute to modified CBF and brain activity but some knowledge gaps remain to understand its exact pathophysiological role [14].

Moreover, considering a dimensional approach, the specificity of alterations highlighted in this review is an important question to raise. For example, SSD and bipolar disorder (BD) are both severe mental illnesses with psychotic features that share significant affective, cognitive and neuroimaging characteristics [92-94]. A recent systematic review of the literature on CBF in BD have reported widespread resting hypoperfusion in the cingulate gyrus, frontal, and anterior temporal regions during acute phases of the disorder when compared to controls [95]. Similarities between the cortical regions hypoperfused in

BD and SSD may suggests a transdiagnostic relation accounting for shared affective or cognitive impairments observed in both disorders. Whether or not this represents an intermediate shared phenotype [96] or a marker of psychosis, it would require a direct comparison to be confirmed. However, increased functional connectivity in the left SFG and fronto-parietal network has started to emerge as a potential endophenotype for SSD serving as a marker to separate patients from healthy [97] and clinical controls [7]. Interestingly, the absence of subcortical findings in the BD literature suggests that hyperperfusion in these regions may also serve as a more specific diagnosis marker of SSD.

In this context, machine learning classification coupled with multimodal brain imaging techniques offers a promising opportunity [98]. Data driven approach can relate multiple clinical, structural, and functional dimensions to provide a comprehensive insight into underlying neurobiology and mechanisms of psychosis. A recent publication conducted with a non-clinical sample of youth presenting sub-psychosis symptoms attempted to classify participants based on ASL and/or BOLD resting-state functional connectivity using support vector [99]. The relative success of the classifier using ASL connectivity changes, complementary to the BOLD changes, raised the specific interest of CBF in predicting psychosis in youth.

Limitations

Our review has some limitations that should be considered. First, the scarcity of perfusion MRI studies in early stages psychosis provided little information regarding CBF alterations associated to CHR and FEP status. Second, outside of the scope of this review were studies exploring the effect of antipsychotic medication on brain perfusion as they usually use clinical control comparisons instead of healthy controls. However, this specific matter has already been addressed in a systematic-review by Goozée et al., (2014), showing that rCBF in basal ganglia and frontal regions appear to be affected by antipsychotics [84]. Considering the potential confounding effect of antipsychotics, longitudinal studies exploring early stages psychosis and antipsychotic-naïve populations are warranted to distinguish the neuroprogressive from the pharmacological nature of perfusion alterations in SSD across time and care. Third, the diversity of the scales used for symptoms assessment prevented us to conduct a meta-regression analysis of rCBF alterations with symptom dimensions. Further rCBF studies specifically investigating the relationship between perfusion alterations and symptomatology are required, not only focusing on positive or negative symptoms, but also on disorganized thinking, abnormal motor behavior, cognitive impairments, and affective symptoms. Fourth, factors known to influence brain perfusion measurements, such as smoking status [100] or arterial transit time (i.e., the time for labeled blood to reach brain tissue) [101, 102], were inconsistently accounted for across studies. While the heterogeneity in

controlled variables and acquisition parameters may have contributed to heterogeneous findings, it also confounds their interpretation. We cannot rule out that results reported here are not better explained by differences in regional and individual sensitivity to ASL imaging. Hence, we urge caution in the interpreting of the present review as significant differences in cortical versus subcortical gray matter, juxtacortical versus periventricular white matter [103], and healthy versus pathological tissue [104, 105] have recently been shown for both arterial transit time and CBF, depending on age and sex. To address this issue, recent multiple post-labeling delays schemes, such as part of the ASL imaging protocol in the Human Connectome Project-Aging [106], are now able to provide robust measures of arterial transit time allowing for optimization of rCBF modeling. In addition, standardization of data acquisition and post-processing methods according to good practice is not only essential to promote comparability but would also improve accuracy and facilitate the interpretation of perfusion findings. First attempts to a standardized approach have been made by Alsop et al., (2015) who provided expert guidelines for ASL acquisition [35] while Clement et al., (2018) have recommended measurement conditions and correction for important confounding variables [100]. Finally, the lack of functional imaging studies of brain perfusion calls for an increased use of vasoactive stimuli such as cognitive tasks or hypercapnia challenge to provide a dynamic perception of neurovascular coupling and cerebrovascular reactivity. Due to the tight relationship between energy demand and supply, perturbations in the brain function and/or structure are likely to be echoed in the brain perfusion and/or vasculature. Whether or not this functional-structural coupling is congruent, represents normalization, overcompensation or continued abnormality, its strength has already shown regional differences [107] that could be better explained by hemodynamic processes. The findings from the present review, including the latter limitations, converge towards the need for multimodal connectivity studies of brain perfusion in SSD. Interestingly, a recent ASL resting state functional connectivity study of youth with early psychosis symptoms have demonstrated the discriminative power of perfusion parameters. ASL imaging holds great promise to the development of individualized and innovant diagnostic and therapeutic approaches with the brain perfusion and the NVU as potential targets [18].

Conclusion

The results of our review and meta-analysis highlight specific patterns of regional CBF in schizophrenia patients compared to HC in relation with the symptomatology. This suggest that CBF is a valid and reliable neuroimaging marker for investigating the physio-pathological correlates of SSD although further research is warranted to explore perfusion at different clinical stages. The cortical regional hypoperfusion and

subcortical hyperperfusion observed support the implication of hemodynamic correlates in relation to the dysconnectivity hypothesis of SSD. The relationship between brain perfusion and dimensions of symptoms is particularly important as it could help better explain clinical heterogeneity and improve outcome prediction.

Declaration of interests

ML reports grants from Otsuka Lundbeck Alliance, diaMentis personal fees from Otsuka Canada, personal fees from Lundbeck Canada, grants and personal fees from Janssen, and personal fees from MedAvante-Prophase, outside the submitted work. Salary awards include Canadian Institutes for Health Research (MC, ML), *Fonds de la Recherche en Santé du Québec* (OP, MC, ML), James McGill Professorship (ML), Quebec Bio-Imaging Network (DRC) and Michal Renata Hornstein in Cardiovascular Imaging (CJG). AM has received fees for lectures at conferences sponsored by Lundbeck and Otsuka, Global in the past and salary awards from Canada Research Chair Program.

Acknowledgements

We would like to thank N. Sukumar, U. Anazodo, and L. Palaniyappan for sharing the quality analysis tool they developed for ASL studies. We would also like to thank S. Shaikh for reviewing the manuscript.

References

1. Van Os J, Linscott RJ, Myin-Germeys I, Delespaul P, Krabbendam LJPm. A systematic review and meta-analysis of the psychosis continuum: evidence for a psychosis proneness-persistence-impairment model of psychotic disorder. 2009;39(2):179.

2. Vos T, Abajobir AA, Abate KH, et al. Global, regional, and national incidence, prevalence, and years lived with disability for 328 diseases and injuries for 195 countries, 1990–2016: a systematic analysis for the Global Burden of Disease Study 2016. *The Lancet* 2017/09/16/ 2017;390(10100):1211-1259.

3. Barch DM, Bustillo J, Gaebel W, et al. Logic and justification for dimensional assessment of symptoms and related clinical phenomena in psychosis: relevance to DSM-5. *Schizophrenia research* 2013;150(1):15-20.

4. Kahn RS, Sommer IE, Murray RM, et al. Schizophrenia. *Nat Rev Dis Primers* Nov 12 2015;1:15067.

5. McGorry PD, Purcell R, Hickie IB, Yung AR, Pantelis C, Jackson HJ. Clinical staging: a heuristic model for psychiatry and youth mental health. *Medical Journal of Australia* 2007;187(S7).

6. Shah JL, Crawford A, Mustafa SS, Iyer SN, Joober R, Malla AK. Is the Clinical High-Risk State a Valid Concept? Retrospective Examination in a First-Episode Psychosis Sample. *Psychiatric Services* 2017;68(10):1046-1052.

7. Brandl F, Avram M, Weise B, et al. Specific Substantial Dysconnectivity in Schizophrenia: A Transdiagnostic Multimodal Meta-analysis of Resting-State Functional and Structural Magnetic Resonance Imaging Studies. *Biol Psychiatry* Apr 1 2019;85(7):573-583.

8. Gao X, Zhang W, Yao L, et al. Association between structural and functional brain alterations in drug-free patients with schizophrenia: a multimodal meta-analysis. *Journal of Psychiatry and Neuroscience* 2018;43(2):131-142.

9. Vanes LD, Mouchlianitis E, Patel K, et al. Neural correlates of positive and negative symptoms through the illness course: an fMRI study in early psychosis and chronic schizophrenia. *Scientific Reports* 2019;9(1).

10. Li M, Deng W, Das T, et al. Neural substrate of unrelenting negative symptoms in schizophrenia: a longitudinal resting-state fMRI study. *European Archives of Psychiatry and Clinical Neuroscience* 2018;268(7):641-651.

11. Gauthier CJ, Fan AP. BOLD signal physiology: Models and applications. *Neuroimage* Feb 15 2019;187:116-127.

12. Chappell M, MacIntosh B, Okell T. *Introduction to perfusion quantification using arterial spin labelling*: Oxford University Press; 2018.

13. Buxton RB. The thermodynamics of thinking: connections between neural activity, energy metabolism and blood flow. *Philosophical transactions of the Royal Society of London Series B, Biological sciences* 2021;376(1815):20190624.

14. Iadecola C. The Neurovascular Unit Coming of Age: A Journey through Neurovascular Coupling in Health and Disease. *Neuron* 2017;96(1):17-42.

15. Kim KJ, Ramiro Diaz J, Iddings JA, Filosa JA. Vasculo-Neuronal Coupling: Retrograde Vascular Communication to Brain Neurons. *The Journal of Neuroscience* 2016;36(50):12624-12639.

16. Moore CI, Cao R. The Hemo-Neural Hypothesis: On The Role of Blood Flow in Information Processing. *Journal of Neurophysiology* 2008;99(5):2035-2047.

17. Baruah J, Vasudevan A. The Vessels Shaping Mental Health or Illness. *Open Neurol J* 2019;13:1-9.

18. Katsel P, Roussos P, Pletnikov M, Haroutunian V. Microvascular anomaly conditions in psychiatric disease. Schizophrenia - angiogenesis connection. *Neurosci Biobehav Rev* Jun 2017;77:327-339.

19. Kety SS, Schmidt CF. The determination of cerebral blood flow in man by the use of nitrous oxide in low concentrations. *American Journal of Physiology* 1945;143:53-66.

20. Hernandez-Garcia L, Aramendía-Vidaurreta V, Bolar DS, et al. Recent Technical Developments in ASL: A Review of the State of the Art. *Magnetic Resonance in Medicine* 2022;88(5):2021-2042.

21. Wintermark M, Sesay M, Barbier E, et al. Comparative Overview of Brain Perfusion Imaging Techniques. *Stroke* 2005;36(9):e83-e99.

22. Fahlström M, Appel L, Kumlien E, et al. Evaluation of Arterial Spin Labeling MRI—Comparison with 15O-Water PET on an Integrated PET/MR Scanner. *Diagnostics* 2021;11(5):821.

23. Bokkers RP, Bremmer JP, Van Berckel BN, et al. Arterial spin labeling perfusion MRI at multiple delay times: a correlative study with H215O positron emission tomography in patients with symptomatic carotid artery occlusion. *Journal of Cerebral Blood Flow & Metabolism* 2010;30(1):222-229.

24. Xu G, Rowley HA, Wu G, et al. Reliability and precision of pseudo-continuous arterial spin labeling perfusion MRI on 3.0 T and comparison with 15O-water PET in elderly subjects at risk for Alzheimer's disease. *NMR in Biomedicine* 2010;23(3):286-293.

25. Detre JA, Rao H, Wang DJ, Chen YF, Wang Z. Applications of arterial spin labeled MRI in the brain. *Journal of Magnetic Resonance Imaging* 2012;35(5):1026-1037.

26. Hendrikse J, Petersen ET, Golay X. Vascular disorders: insights from arterial spin labeling. *Neuroimaging Clinics* 2012;22(2):259-269.

27. Ferré JC, Bannier E, Raoult H, Mineur G, Carsin-Nicol B, Gauvrit JY. Arterial spin labeling (ASL) perfusion: Techniques and clinical use. *Diagnostic and Interventional Imaging* 2013;94(12):1211-1223.

28. Haller S, Zaharchuk G, Thomas DL, Lovblad K-O, Barkhof F, Golay X. Arterial Spin Labeling Perfusion of the Brain: Emerging Clinical Applications. *Radiology* 2016;281(2):337-356.

29. Giovacchini G, Squitieri F, Esmaeilzadeh M, Milano A, Mansi L, Ciarmiello A. PET translates neurophysiology into images: A review to stimulate a network between neuroimaging and basic research. *J Cell Physiol* Apr 2011;226(4):948-961.

30. Ingvar D, Franzén G. DISTRIBUTION OF CEREBRAL ACTIVITY IN CHRONIC SCHIZOPHRENIA. *The Lancet* 1974;304(7895):1484-1486.

31. Hill K, Mann L, Laws KR, Stephenson CME, Nimmo-Smith I, McKenna PJ. Hypofrontality in schizophrenia: a meta-analysis of functional imaging studies. *Acta Psychiatrica Scandinavica* 2004;110(4):243-256.

32. van Erp TGM, Walton E, Hibar DP, et al. Cortical Brain Abnormalities in 4474 Individuals With Schizophrenia and 5098 Control Subjects via the Enhancing Neuro Imaging Genetics Through Meta Analysis (ENIGMA) Consortium. *Biol Psychiatry* Nov 1 2018;84(9):644-654.

33. Catafau AM, Parellada E, Lomeña FJ, Bernardo M, Pavía J, Ros D, Setoain J, Gonzalez-Monclús E. Prefrontal and temporal blood flow in schizophrenia: resting and activation technetium-99m-HMPAO SPECT patterns in young neuroleptic-naive patients with acute disease. *Journal of nuclear medicine : official publication, Society of Nuclear Medicine* 1994;35(6):935-941.

34. Guimarães TM, Machado-de-Sousa JP, Crippa JAS, Guimarães MRC, Hallak JEC. Arterial spin labeling in patients with schizophrenia: a systematic review. *Archives of Clinical Psychiatry (São Paulo)* 2016;43(6):151-156.

35. Alsop DC, Detre JA, Golay X, et al. Recommended implementation of arterial spin-labeled perfusion MRI for clinical applications: A consensus of the ISMRM perfusion study group and the European consortium for ASL in dementia. *Magnetic Resonance in Medicine* 2015;73(1):102-116.

36. Page MJ, McKenzie JE, Bossuyt PM, et al. The PRISMA 2020 statement: an updated guideline for reporting systematic reviews. *BMJ* 2021:n71.

37. Sukumar N, Sabesan P, Anazodo U, Palaniyappan L. Neurovascular Uncoupling in Schizophrenia: A Bimodal Meta-Analysis of Brain Perfusion and Glucose Metabolism. *Frontiers in Psychiatry* 2020;11.

38. Welker K, Boxerman J, Kalnin A, Kaufmann T, Shiroishi M, Wintermark M. ASFNR Recommendations for Clinical Performance of MR Dynamic Susceptibility Contrast Perfusion Imaging of the Brain. *American Journal of Neuroradiology* 2015;36(6):E41-E51.

39. Albajes-Eizagirre A, Solanes A, Vieta E, Radua J. Voxel-based meta-analysis via permutation of subject images (PSI): Theory and implementation for SDM. *Neuroimage* 2019-02-01 2019;186:174-184.

40. Radua J, Mataix-Cols D, Phillips ML, El-Hage W, Kronhaus DM, Cardoner N, Surguladze S. A new meta-analytic method for neuroimaging studies that combines reported peak coordinates and statistical parametric maps. *European Psychiatry* 2012/11/01/ 2012;27(8):605-611.

41. Friedman L, Turner JA, Stern H, Mathalon DH, Trondsen LC, Potkin SG. Chronic smoking and the BOLD response to a visual activation task and a breath hold task in patients with schizophrenia and healthy controls. 2008;40(3):1181-1194.

42. Foucher JR, Zhang YF, Roser M, et al. A double dissociation between two psychotic phenotypes: Periodic catatonia and cataphasia. *Prog Neuropsychopharmacol Biol Psychiatry* Aug 30 2018;86:363-369.

43. Liu J, Qiu M, Constable RT, Wexler BE. Does baseline cerebral blood flow affect task-related blood oxygenation level dependent response in schizophrenia? *Schizophr Res* Sep 2012;140(1-3):143-148.

44. Squarcina L, Perlini C, Peruzzo D, et al. The use of dynamic susceptibility contrast (DSC) MRI to automatically classify patients with first episode psychosis. *Schizophr Res* Jun 2015;165(1):38-44.

45. Cui LB, Wang LX, Tian P, et al. Aberrant perfusion and its connectivity within default mode network of first-episode drug-naive schizophrenia patients and their unaffected first-degree relatives. *Sci Rep* Nov 23 2017;7(1):16201.

46. Mäntylä T, Kieseppä T, Suvisaari J, Raij TT. Delineating insight-processing-related functional activations in the precuneus in first-episode psychosis patients. *Psychiatry Research: Neuroimaging* 2021/11/30/ 2021;317:111347.

47. Chen J, Xue K, Yang M, et al. Altered Coupling of Cerebral Blood Flow and Functional Connectivity Strength in First-Episode Schizophrenia Patients With Auditory Verbal Hallucinations. *Frontiers in Neuroscience* 2022-April-25 2022;16.

48. Allen P, Azis M, Modinos G, et al. Increased Resting Hippocampal and Basal Ganglia Perfusion in People at Ultra High Risk for Psychosis: Replication in a Second Cohort. *Schizophr Bull* Oct 17 2018;44(6):1323-1331.

49. Allen P, Chaddock CA, Egerton A, et al. Resting hyperperfusion of the hippocampus, midbrain, and basal ganglia in people at high risk for psychosis. *American Journal of Psychiatry* 01 Apr 2016;173(4):392-399.

50. Modinos G, Richter A, Egerton A, et al. Interactions between hippocampal activity and striatal dopamine in people at clinical high risk for psychosis: relationship to adverse outcomes. *Neuropsychopharmacology* 2021.

51. Pinkham A, Loughead J, Ruparel K, Wu WC, Overton E, Gur R. Resting quantitative cerebral blood flow in schizophrenia measured by pulsed arterial spin labeling perfusion MRI. *Psychiatry Research - Neuroimaging* 31 October 2011;194(1):64-72.

52. Zhu J, Zhuo C, Qin W, Xu Y, Xu L, Liu X, Yu C. Altered resting-state cerebral blood flow and its connectivity in schizophrenia. *J Psychiatr Res* Apr 2015;63:28-35.

53. Schneider K, Michels L, Hartmann-Riemer MN, et al. Cerebral blood flow in striatal regions is associated with apathy in patients with schizophrenia. *J Psychiatry Neurosci* Mar 1 2019;44(2):102-110.

54. Khalil M, Hollander P, Raucher-Chene D, Lepage M, Lavigne KM. Structural brain correlates of cognitive function in schizophrenia: A meta-analysis. *Neurosci Biobehav Rev* Jan 2022;132:37-49.

55. Jimenez AM, Riedel P, Lee J, Reavis EA, Green MF. Linking resting-state networks and social cognition in schizophrenia and bipolar disorder. *Human Brain Mapping* 2019;40(16):4703-4715.

56. Pelletier-Baldelli A, Holt DJ. Chapter Five - Shared neural substrates of deficits in social cognition and negative symptoms in schizophrenia. In: Lewandowski KE, Moustafa AA, eds. *Social Cognition in Psychosis*: Academic Press; 2019:125-142.

57. Pokorny VJ, Lano TJ, Schallmo M-P, Olman CA, Sponheim SR. Reduced influence of perceptual context in schizophrenia: behavioral and neurophysiological evidence. *Psychological Medicine* 2021;51(5):786-794.

58. Javitt DC. Sensory Processing in Schizophrenia: Neither Simple nor Intact. *Schizophrenia Bulletin* 2009;35(6):1059-1064.

59. Zhuo C, Tian H, Fang T, et al. Neural mechanisms underlying visual and auditory processing impairments in schizophrenia: insight into the etiology and implications for tailoring preventive and therapeutic interventions. *Am J Transl Res* 2020;12(12):7657-7669.

60. Hovington CL, Lepage M. Neurocognition and neuroimaging of persistent negative symptoms of schizophrenia. *Expert review of neurotherapeutics* 2012;12(1):53-69.

61. Venkatasubramanian G. Neuroanatomical correlates of psychopathology in antipsychotic-naive schizophrenia. *Indian journal of psychiatry* 2010;52(1):28.

62. Benoit A, Bodnar M, Malla AK, Joober R, Lepage M. The Structural Neural Substrates of Persistent Negative Symptoms in First-Episode of Non-Affective Psychosis: A Voxel-Based Morphometry Study. *Frontiers in psychiatry* 2012;3:42.

63. Bodnar M, Hovington CL, Buchy L, Malla AK, Joober R, Lepage M. Cortical Thinning in Temporo-Parietal Junction (TPJ) in Non-Affective First-Episode of Psychosis Patients with Persistent Negative Symptoms. *Plos One* Jun 2014;9(6).

64. Millan MJ, Fone K, Steckler T, Horan WP. Negative symptoms of schizophrenia: clinical characteristics, pathophysiological substrates, experimental models and prospects for improved treatment. *European neuropsychopharmacology* 2014;24(5):645-692.

65. Xu L, Qin W, Zhuo C, Liu H, Zhu J, Yu C. Combination of volume and perfusion parameters reveals different types of grey matter changes in schizophrenia. *Sci Rep* Mar 27 2017;7(1):435.

66. Radua J, Borgwardt S, Crescini A, Mataix-Cols D, Meyer-Lindenberg A, McGuire PK, Fusar-Poli P. Multimodal meta-analysis of structural and functional brain changes in first episode psychosis and the effects of antipsychotic medication. *Neuroscience & Biobehavioral Reviews* 2012;36(10):2325-2333.

67. Kirschner M, Haugg A, Manoliu A, Simon JJ, Huys QJM, Seifritz E, Tobler PN, Kaiser S. Deficits in context-dependent adaptive coding in early psychosis and healthy individuals with schizotypal personality traits. *Brain* 2018;141(9):2806-2819.

68. Soldevila-Matías P, Albajes-Eizagirre A, Radua J, et al. Precuneus and insular hypoactivation during cognitive processing in first-episode psychosis: Systematic review and meta-analysis of fMRI studies. *Rev Psiquiatr Salud Ment (Engl Ed)* Sep 25 2020.

69. İnce E, Üçok A. Relationship Between Persistent Negative Symptoms and Findings of Neurocognition and Neuroimaging in Schizophrenia. *Clinical EEG and Neuroscience* 2018;49(1):27-35.

70. Najas-Garcia A, Gómez-Benito J, Huedo-Medina TB. The Relationship of Motivation and Neurocognition with Functionality in Schizophrenia: A Meta-analytic Review. *Community Mental Health Journal* 2018;54(7):1019-1049.

71. Halverson TF, Orleans-Pobee M, Merritt C, Sheeran P, Fett AK, Penn DL. Pathways to functional outcomes in schizophrenia spectrum disorders: Meta-analysis of social cognitive and neurocognitive predictors. *Neuroscience and Biobehavioral Reviews* Oct 2019;105:212-219.

72. Ventura J, Hellemann GS, Thames AD, Koellner V, Nuechterlein KH. Symptoms as mediators of the relationship between neurocognition and functional outcome in schizophrenia: A meta-analysis. *Schizophrenia Research* Sep 2009;113(2-3):189-199.

73. Ventura J, Wood RC, Hellemann GS. Symptom Domains and Neurocognitive Functioning Can Help Differentiate Social Cognitive Processes in Schizophrenia: A Meta-Analysis. *Schizophrenia Bulletin* 2013;39(1):102-111.

74. Lin C-H, Huang C-L, Chang Y-C, Chen P-W, Lin C-Y, Tsai GE, Lane H-Y. Clinical symptoms, mainly negative symptoms, mediate the influence of neurocognition and social cognition on functional outcome of schizophrenia. *Schizophrenia Research* 2013;146(1-3):231-237.

75. Cantisani A, Stegmayer K, Federspiel A, Bohlhalter S, Wiest R, Walther S. Blood perfusion in left inferior and middle frontal gyrus predicts communication skills in schizophrenia. *Psychiatry Res Neuroimaging* Apr 30 2018;274:7-10.

76. Wojtalik JA, Smith MJ, Keshavan MS, Eack SM. A Systematic and Meta-analytic Review of Neural Correlates of Functional Outcome in Schizophrenia. *Schizophrenia Bulletin* 2017-10-21 2017;43(6):1329-1347.

77. Brugger SP, Howes OD. Heterogeneity and Homogeneity of Regional Brain Structure in Schizophrenia: A Meta-analysis. *JAMA Psychiatry* Nov 1 2017;74(11):1104-1111.

78. Howes OD, Kapur S. The dopamine hypothesis of schizophrenia: version III—the final common pathway. *Schizophrenia bulletin* 2009;35(3):549-562.

79. Howes OD, Murray RM. Schizophrenia: an integrated sociodevelopmental-cognitive model. *Lancet* May 10 2014;383(9929):1677-1687.

80. Brugger SP, Angelescu I, Abi-Dargham A, Mizrahi R, Shahrezaei V, Howes OD. Heterogeneity of Striatal Dopamine Function in Schizophrenia: Meta-analysis of Variance. *Biological Psychiatry* 2020;87(3):215-224.

81. Nelson AB, Kreitzer AC. Reassessing models of basal ganglia function and dysfunction. *Annual review of neuroscience* 2014;37:117-135.

82. Cui L-B, Liu L, Guo F, et al. Disturbed Brain Activity in Resting-State Networks of Patients with First-Episode Schizophrenia with Auditory Verbal Hallucinations: A Cross-sectional Functional MR Imaging Study. *Radiology* 2017;283(3):810-819.

83. Raij TT, Mäntylä T, Kieseppä T, Suvisaari J. Aberrant functioning of the putamen links delusions, antipsychotic drug dose, and compromised connectivity in first episode psychosis—Preliminary fMRI findings. *Psychiatry Research: Neuroimaging* 2015;233(2):201-211.

84. Goozée R, Handley R, Kempton MJ, Dazzan P. A systematic review and meta-analysis of the effects of antipsychotic medications on regional cerebral blood flow (rCBF) in schizophrenia: Association with response to treatment. 2014;43:118-136.

85. Lahti AC, Weiler MA, Holcomb HH, Tamminga CA, Cropsey KL. Modulation of limbic circuitry predicts treatment response to antipsychotic medication: a functional imaging study in schizophrenia. *Neuropsychopharmacology* Dec 2009;34(13):2675-2690.

86. Rodríguez VM, Andrée RM, Pérez Castejón MJ, Catalina Zamora ML, Alvaro PC, Carreras Delgado JL, Rubia Vila FJ. Fronto-striato-thalamic perfusion and clozapine response in treatment-refractory schizophrenic patients. A99mTc-HMPAO study. *Psychiatry Research: Neuroimaging* 1997;76(1):51-61.

87. Scheef L, Manka C, Daamen M, Kuhn KU, Maier W, Schild HH, Jessen F. Resting-state perfusion in nonmedicated schizophrenic patients: a continuous arterial spin-labeling 3.0-T MR study. *Radiology* Jul 2010;256(1):253-260.

88. Zhao C, et al. Structural and functional brain abnormalities in schizophrenia: A cross-sectional study at different stages of the disease. *Progress in Neuro-Psychopharmacology and Biological Psychiatry* 2018;83:27.

89. Cui LB, Chen G, Xu ZL, et al. Cerebral blood flow and its connectivity features of auditory verbal hallucinations in schizophrenia: A perfusion study. *Psychiatry Res Neuroimaging* Feb 28 2017;260:53-61.

90. Oliveira IAF, Guimaraes TM, Souza RM, Dos Santos AC, Machado-de-Sousa JP, Hallak JEC, Leoni RF. Brain functional and perfusional alterations in schizophrenia: an arterial spin labeling study. *Psychiatry Res Neuroimaging* Feb 28 2018;272:71-78.

91. Gong Q, Puthusseryppady V, Dai J, et al. Dysconnectivity of the medio-dorsal thalamic nucleus in drug-naive first episode schizophrenia: diagnosis-specific or trans-diagnostic effect? *Transl Psychiatry* Jan 16 2019;9(1):9.

92. Bortolato B, Miskowiak KW, Kohler CA, Vieta E, Carvalho AF. Cognitive dysfunction in bipolar disorder and schizophrenia: a systematic review of meta-analyses. *Neuropsychiatr Dis Treat* 2015;11:3111-3125.

93. Smucny J, Iosif A-M, Eaton NR, et al. Latent Profiles of Cognitive Control, Episodic Memory, and Visual Perception Across Psychiatric Disorders Reveal a Dimensional Structure. *Schizophrenia Bulletin* 2019;46(1):154-162.

94. McTeague LM, Huemer J, Carreon DM, Jiang Y, Eickhoff SB, Etkin A. Identification of Common Neural Circuit Disruptions in Cognitive Control Across Psychiatric Disorders. *Am J Psychiatry* Jul 1 2017;174(7):676-685.

95. Toma S, MacIntosh BJ, Swardfager W, Goldstein BI. Cerebral blood flow in bipolar disorder: A systematic review. *J Affect Disord* Dec 1 2018;241:505-513.

96. Ivleva EI, Clementz BA, Dutcher AM, et al. Brain Structure Biomarkers in the Psychosis Biotypes: Findings From the Bipolar-Schizophrenia Network for Intermediate Phenotypes. *Biological Psychiatry* 2017;82(1):26-39.

97. Ding Y, Ou Y, Su Q, et al. Enhanced Global-Brain Functional Connectivity in the Left Superior Frontal Gyrus as a Possible Endophenotype for Schizophrenia. *Frontiers in Neuroscience* 2019-February-26 2019;13.

98. Du Y, Fu Z, Calhoun VD. Classification and Prediction of Brain Disorders Using Functional Connectivity: Promising but Challenging. *Front Neurosci* 2018;12:525.

99. Overton DJ, Bhagwat N, Viviano JD, Jacobs GR, Voineskos AN. Identifying psychosis spectrum youth using support vector machines and cerebral blood perfusion as measured by arterial spin labeled fMRI. *Neuroimage Clin* Jun 4 2020;27:102304.

100. Clement P, Petr J, Dijsselhof MBJ, et al. A Beginner's Guide to Arterial Spin Labeling (ASL) Image Processing. *Frontiers in Radiology* 2022-June-14 2018;2.

101. Petersen ET, Mouridsen K, Golay X. The QUASAR reproducibility study, Part II: Results from a multi-center Arterial Spin Labeling test–retest study. *Neuroimage* 2010;49(1):104-113.

102. Bokkers R, Van Der Worp H, Mali W, Hendrikse J. Noninvasive MR imaging of cerebral perfusion in patients with a carotid artery stenosis. *Neurology* 2009;73(11):869-875.

103. Juttukonda MR, Li B, Almaktoum R, Stephens KA, Yochim KM, Yacoub E, Buckner RL, Salat DH. Characterizing cerebral hemodynamics across the adult lifespan with arterial spin labeling MRI data from the Human Connectome Project-Aging. *Neuroimage* 2021/04/15/ 2021;230:117807.

104. Hendrikse J, van Osch MJ, Rutgers DR, Bakker CJ, Kappelle LJ, Golay X, van der Grond J. Internal carotid artery occlusion assessed at pulsed arterial spin-labeling perfusion MR imaging at multiple delay times. *Radiology* 2004;233(3):899-904.

105. Hirschler L, Munting LP, Khmelinskii A, et al. Transit time mapping in the mouse brain using time-encoded pCASL. *NMR in Biomedicine* 2018;31(2):e3855.

106. Harms MP, Somerville LH, Ances BM, et al. Extending the Human Connectome Project across ages: Imaging protocols for the Lifespan Development and Aging projects. *Neuroimage* 2018;183:972-984.

107. Preti MG, Van De Ville D. Decoupling of brain function from structure reveals regional behavioral specialization in humans. *Nat Commun* Oct 18 2019;10(1):4747.

108. Bellani M, Peruzzo D, Isola M, et al. Cerebellar and lobar blood flow in schizophrenia: a perfusion weighted imaging study. *Psychiatry Res* Jul 30 2011;193(1):46-52.

109. Homan P, Kindler J, Hauf M, Walther S, Hubl D, Dierks T. Repeated measurements of cerebral blood flow in the left superior temporal gyrus reveal tonic hyperactivity in patients with auditory verbal hallucinations: a possible trait marker. *Front Hum Neurosci* 2013;7(JUN):304.

110. Horn H, Federspiel A, Wirth M, Muller TJ, Wiest R, Wang JJ, Strik W. Structural and metabolic changes in language areas linked to formal thought disorder. *Br J Psychiatry* Feb 2009;194(2):130-138.

111. Jing R, Huang J, Jiang D, Lin X, Ma X, Tian H, Li J, Zhuo C. Distinct pattern of cerebral blood flow alterations specific to schizophrenics experiencing auditory verbal hallucinations with and without insight: a pilot study. *Oncotarget* Jan 23 2018;9(6):6763-6770.

112. Kim J, Plitman E, Nakajima S, et al. Modulation of brain activity with transcranial direct current stimulation: Targeting regions implicated in impaired illness awareness in schizophrenia. *Eur Psychiatry* Sep 2019;61:63-71.

113. Kindler J, Jann K, Homan P, Hauf M, Walther S, Strik W, Dierks T, Hubl D. Static and dynamic characteristics of cerebral blood flow during the resting state in schizophrenia. *Schizophrenia Bulletin* 01 Jan 2015;41(1):163-170.

114. Kindler J, Schultze-Lutter F, Hauf M, Dierks T, Federspiel A, Walther S, Schimmelmann BG, Hubl D. Increased Striatal and Reduced Prefrontal Cerebral Blood Flow in Clinical High Risk for Psychosis. *Schizophr Bull* Jan 13 2018;44(1):182-192.

115. Legind CS, Broberg BV, Brouwer R, et al. Heritability of Cerebral Blood Flow and the Correlation to Schizophrenia Spectrum Disorders: A Pseudo-continuous Arterial Spin Labeling Twin Study. *Schizophr Bull* Oct 24 2019;45(6):1231-1241.

116. Ma X, Wang D, Zhou Y, Zhuo C, Qin W, Zhu J, Yu C. Sex-dependent alterations in resting-state cerebral blood flow, amplitude of low-frequency fluctuations and their coupling relationship in schizophrenia. *Aust N Z J Psychiatry* Apr 2016;50(4):334-344.

117. Modinos G, Richter A, Egerton A, et al. Interactions between hippocampal activity and striatal dopamine in people at clinical high risk for psychosis: relationship to adverse outcomes. *Neuropsychopharmacology* 2021;46(8):1468-1474.

118. Ota M, Ishikawa M, Sato N, et al. Pseudo-continuous arterial spin labeling MRI study of schizophrenic patients. *Schizophr Res* Apr 2014;154(1-3):113-118.

119. Ota M, Sato N, Sakai K, et al. Altered coupling of regional cerebral blood flow and brain temperature in schizophrenia compared with bipolar disorder and healthy subjects. *J Cereb Blood Flow Metab* Dec 2014;34(12):1868-1872.

120. Peruzzo D, Rambaldelli G, Bertoldo A, et al. The impact of schizophrenia on frontal perfusion parameters: a DSC-MRI study. *J Neural Transm (Vienna)* Apr 2011;118(4):563-570.

121. Pillinger T, Rogdaki M, McCutcheon RA, Hathway P, Egerton A, Howes OD. Altered glutamatergic response and functional connectivity in treatment resistant schizophrenia: the effect of riluzole and therapeutic implications. *Psychopharmacology (Berl)* Jul 2019;236(7):1985-1997.

122. Pinkham A, Loughead J, Ruparel K, Wu WC, Overton E, Gur R, Gur R. Resting quantitative cerebral blood flow in schizophrenia measured by pulsed arterial spin labeling perfusion MRI. *Psychiatry Res* Oct 31 2011;194(1):64-72.

123. Pinkham AE, Liu P, Lu H, Kriegsman M, Simpson C, Tamminga C. Amygdala Hyperactivity at Rest in Paranoid Individuals With Schizophrenia. *Am J Psychiatry* Aug 1 2015;172(8):784-792.

124. Stegmayer K, et al. Specific cerebral perfusion patterns in three schizophrenia symptom dimensions. *Schizophrenia Research* 2017;190:96.

125. Stegmayer K, Stettler M, Strik W, Federspiel A, Wiest R, Bohlhalter S, Walther S. Resting state perfusion in the language network is linked to formal thought disorder and poor functional outcome in schizophrenia. *Acta Psychiatr Scand* Nov 2017;136(5):506-516.

126. Talati P, Rane S, Skinner J, Gore J, Heckers S. Increased hippocampal blood volume and normal blood flow in schizophrenia. *Psychiatry Res* Jun 30 2015;232(3):219-225.

127. Walther S, Federspiel A, Horn H, Razavi N, Wiest R, Dierks T, Strik W, Muller TJ. Resting state cerebral blood flow and objective motor activity reveal basal ganglia dysfunction in schizophrenia. *Psychiatry Res* May 31 2011;192(2):117-124.

128. Walther S, Schappi L, Federspiel A, Bohlhalter S, Wiest R, Strik W, Stegmayer K. Resting-State Hyperperfusion of the Supplementary Motor Area in Catatonia. *Schizophr Bull* Sep 1 2017;43(5):972-981.

129. Wijtenburg SA, Wright SN, Korenic SA, et al. Altered Glutamate and Regional Cerebral Blood Flow Levels in Schizophrenia: A 1 H-MRS and pCASL study. *Neuropsychopharmacology* 01 Jan 2017;42(2):562-571.

130. Wright S, Kochunov P, Chiappelli J, et al. Accelerated white matter aging in schizophrenia: role of white matter blood perfusion. *Neurobiol Aging* Oct 2014;35(10):2411-2418.

131. Wright SN, Hong LE, Winkler AM, et al. Perfusion shift from white to gray matter may account for processing speed deficits in schizophrenia. *Hum Brain Mapp* Oct 2015;36(10):3793-3804.

132. Zhu J, Zhuo C, Liu F, Xu L, Yu C. Neural substrates underlying delusions in schizophrenia. *Sci Rep* Sep 21 2016;6:33857.

133. Zhu J, Zhuo C, Xu L, Liu F, Qin W, Yu C. Altered Coupling Between Resting-State Cerebral Blood Flow and Functional Connectivity in Schizophrenia. *Schizophr Bull* Oct 21 2017;43(6):1363-1374.

134. Zhuo C, Zhu J, Qin W, Qu H, Ma X, Yu C. Cerebral blood flow alterations specific to auditory verbal hallucinations in schizophrenia. *Br J Psychiatry* Mar 2017;210(3):209-215.

	Basic principle	+	-	Recommendations
Dynamic Susceptibility Contrast (DSC)	• intravenous injection of an exogenous paramagnetic contrast agent (typically gadolinium-based) • serial measurement of the regional susceptibility-induced signal loss in T2/T2*-weighted images	• clinical indications (e.g. brain tumors, acute inflamation, cerebrovascular disorders) • non-ionizing radiations • measure several hemodynamic parameters (e.g., CBF, CBV, MTT, TTP)	• invasive • sensitive to signal loss due to artifact • abolute quantification of hemodynamic parameters depend on the deconvolution method of the perfusion-weithed imaging data (no consensus)	American Society of Functional Neuroradiology (Welker et al., 2015)
Arterial Spin Labelling (ASL)	• magnetic labelisation of arterial blood water protons (i.e., spins) as an endogenous tracer • delay to let the labelled blood-water flow through the neurovasculature • acquisition of multiple pairs of label and control images	• non-invasive • non-ionizing radiations • quantitative measure of absolute perfusion	• sensitive to motion • requirement for a high signal to noise ratio • possible inaccuracy of measurement in the context of high or low CBF	International Society for Magnetic Resonance in Medicine Perfusion Study Group and the European Consortium for ASL in Dementia (Alsop et al., 2015)
CASL: continuous ASL				
pASL: pulse ASL				
pCASL: pseudocontinuous ASL				

Table 1. Comparison of MRI-based perfusion methods.
Abbreviations: CBF = cerebral blod flow; CBV = cerebral brain voume; MTT = mean-transit-time; TTP = time-to-peak.

Stages	Authors	Population	N	Sex (M/F)	Age (SD)	PANSS (SD)	CPZeq (SD)	Years of illness (SD)	MRI Sequence	T	Analysis	Perfusion outcome	Significant differences (ROIs)	Quality
Arterial spin labelling														
	Stegmayer et al., 2017a [125]	SSD	47	29/18	38.2 (11.4)	72.6 (17.1)	400.2 (344.2)	12.2 (12.3)	pCASL	3	WB	resting-state rCBF	HC > SSD (10)	1.00
	Pinkham et al., 2015 [123]	SZ, SZA; paranoia +/-	32	19/13	38.7 (10.8)	15.9 (3.5)	341.4 (467.4)	NR	pCASL	3	WB	resting-state rCBF	HC > SSD (4); SSD > HC (1); HC > paranoia + (1); paranoia + > HC (2); paranoia - > HC (1)	1.00
	Oliveira et al., 2018 [90]	SZ	28	24/4	32.8 (7.8)	69.4 (17.2)	NR	14.3 (8.3)	pCASL	3	WB	resting-state rCBF	HC > SSD (12); SSD > HC (5)	0.97
	Pinkham et al., 2011 [122]	SZ, SZA	30	18/12	36.7 (10.3)	NR	373.7 (333.4)	NR	PASL-QUIPSSII	3	WB	resting-state rCBF	HC > SSD (5); SSD > HC (4)	0.93
	Kindler et al., 2015 * [113]	SSD	34	18/16	41.5 (12.9)	75.5 (17.3)	518.9 (235.7)	NR	pCASL	3	WB	resting-state rCBF	HC > SSD (2)	0.90
	Walther et al., 2011 [127]	SZ	11	8/3	35.4 (12.5)	54.3 (14.1)	442.6 (241.0)	8.9 (13.3)	PASL-QUIPSSII	3	WB	resting-state rCBF	HC > SSD (5)	0.90
	Ota et al., 2014a [118]	SZ	36	17/19	39.8 (12.6)	61.8 (19.3)	604.8 (459.2)	16.8 (11.3)	pCASL	3	WB	resting-state rCBF	HC > SSD (3)	0.87
	Scheef et al., 2010 [87]	SZ	11	8/3	32.0 (5.0)	43.1 (8.5)	Drugnaive	NR	CASL	3	WB	resting-state rCBF	HC > SSD (8); SSD > HC (6)	0.87
	Homan et al., 2013 + [109]	SZ, SZA	11	3/8	37.1 (8.8)	67.1 (18.9)	714.5 (475.5)	NR	pCASL	3	ROI	resting-state rCBF	SSD > HC (1)	0.83
	Horn et al., 2009 [110]	SZ	13	8/5	29.6 (11.2)	63.9 (16.7)	556.2 (NR)	2.8 (2.6)	PASL-QUIPSSII	1.5	WB	resting-state rCBF	NS	0.83
	Zhu et al., 2015 ▲ [52]	SZ	100	57/43	33.6 (8.6)	71.3 (22.7)	453.2 (342.9)	0.9 (0.7)	pCASL	3	WB	resting-state rCBF	HC > SSD (5); SSD > HC (6)	0.77
	*Stegmayer et al., 2017b** [124]	SSD	47	29/18	38.8 (13.6)	72.6 (17.1)	400.2 (344.2)	7.2 (7.1)	pCASL	3	WB	resting-state rCBF	HC > SSD (2)	0.70
	Kindler et al., 2018 + [114]	SZ, SZA	32	18/14	41.6 (13.4)	76.6 (17.4)	497.0 (210.0)	NR	pCASL	3	WB	resting-state rCBF	SSD > HC (1); HC > SSD (3)	0.70
	Zhu et al., 2017 ▲ [133]	SZ	89	49/40	33.5 (7.8)	71.1 (23.6)	458.9 (343.3)	9.8 (7.6)	pCASL	3	WB	resting-state rCBF	HC > SSD (6); SSD > HC (6)	0.70
	*Wright et al., 2014** [130]	SZ	50	31/19	36.9 (13.4)	NR	629.0 (653.0)	19.1 (12.9)	pCASL	3	WB	resting-state global CBF	NS	0.70
	Zhuo et al., 2017 ▲ [134]	SZ; AVH +/-	76	45/31	31.9 (6.7)	70.6 (23.3)	470.5 (329.1)	9.3 (6.9)	pCASL	3	WB	resting-state rCBF	HC > AVH + (6); AVH + > HC (8); HC > AVH - (5); AVH - > HC (7)	0.70
SSD	*Zhu et al., 2016* [132]	SZ; delusion +/-	49	26/23	35.4 (9.3)	67.1 (18.9)	483.7 (368.0)	11.1 (8.8)	pCASL	3	WB	resting-state rCBF	HC > delusion + (5); delusion + > HC (1); HC > delusion - (5); delusion - > HC (1)	0.70
	Kim et al., 2019 [112]	SZ, SZA	12	7/5	45.0 (12.1)	NR	492.1 (184.9)	19.6 (12.9)	pCASL	3	WB	resting-state rCBF	HC > SSD (2)	0.67
	Schneider et al., 2019 [53]	SZ	29	22/7	27.7 (7.2)	47.7 (10.2)	497.7 (407.4)	7.2 (7.1)	pCASL	3	ROI	resting-state rCBF	NS	0.67
	*Wright et al., 2015** [131]	SZ	46	30/16	37.5 (13.4)	NR	NR	19.5 (13.5)	pCASL	3	WB	resting-state global CBF	HC > SSD (3)	0.67
	Cui et al., 2017a [89]	SZ; AVH +/-	50	27/23	24.0 (6.1)	100.5 (17.7)	NR	9.6 (14.9)	PASL-PICORE	3	WB	resting-state rCBF	HC > AVH + (10); HC > AVH - (1)	0.67
	Walther et al., 2017* [128]	SZ; catatonia +/-	42	28/14	36.7 (11.4)	70.7 (17.3)	404.9 (354.9)	11.3 (10.9)	pCASL	3	WB	resting-state rCBF	HC > SSD (3) catatonia + > catatonia - (2)	0.67
	Legind et al., 2019 [115]	SSD; MZ/DZ	45	28/17	40.6 (9.7)	60.1 (19.0)	NR	14.2 (8.0)	pCASL	3	ROI	resting-state rCBF	SSD > HC (5)	0.63
	Jing et al., 2018 [111]	SZ; insight +/-	18	8/10	33.5 (10.7)	70.4 (19.4)	374.7 (188.0)	11.3 (8.3)	pCASL	3	WB	resting-state rCBF	HC > insight + (8); insight - > HC (5)	0.63
	Ma et al., 2016 ▲ [116]	SZ; male/female	95	51/44	33.6 (8.4)	71.5 (23.2)	453.5 (345.6)	9.9 (7.6)	pCASL	3	WB	resting-state rCBF	HC m > SSD m (3); HC f > SSD f (12); SSD f > HC f (8)	0.63
	*Wijtenburg et al., 2017** [129]	SZ; younger/older	95	60/35	37.2 (5.0)	NR	NR	15.6 (7.7)	pCASL	3	ROI	resting-state rCBF	NS	0.63
	Xu et al., 2017 ▲ [64]	SZ	100	58/42	34.1 (8.2)	108.3 (25.7)	451.8 (342.3)	10.5 (8.1)	pCASL	3	WB	resting-state rCBF	HC > SSD (4); SSD > HC (2)	0.63
	Liu et al., 2012 [63]	SZ, SZA	19	11/8	NR	NR	622.1 (418.0)	20.5 (10.0)	PASL-QUIPSSII	3	WB	resting-state rCBF face processing task NVC	HC > SSD (2); SSD > HC (1)	0.60
	Foucher et al., 2018 [62]	SZ, SZA; catatonia/cataphasia	29	14/15	38.0 (11.6)	66.0 (14.6)	12.7 (10.9)	15.2 (11.2)	PASL-QUIPSSII	3	WB	cognitive task rCBF	SSD > HC (2); catatonia > HC (5); HC > cataphasia (3)	0.60
	Pillinger et al., 2019 [121]	TRS	19	16/3	39.7 (10.9)	72.5 (10.2)	NR	NR	pCASL	3	ROI	resting-state rCBF	NS	0.57
	Ota et al., 2014b [119]	SZ	22	19/3	36.3 (10.4)	65.2 (13.3)	573.9 (470.8)	NR	pCASL	3	WB	resting-state rCBF	NR	0.57
	Cui et al., 2017b [45]	FES	45	25/20	26.8 (5.6)	96.0 (18.0)	Drugnaive	NR	PASL	3	WB	resting-state rCBF	FES > HC (2)	0.73
FEP	Chen et al., 2022 [47]	FES; AVH +/-	85	39/46	21.0 (7.6)	82.0 (15.4)	Drugnaive	NR	pCASL	3	WB	resting-state rCBF	HC > FES (5); FES > HC (2) HC > AVH + (3); AVH - > HC (6) HC > AVH - (1)	0.63
	Mäntylä et al., 2021 [46]	FEP	19	17/2	24.8 (NR)	41.0 (NR)	341.7 (NR)	NR	PASL-Q2TIPS	3	WB	resting-state rCBF	NS	0.87
	Modinos et al., 2021 ○ [117]	CHR	67	40/27	22.8 (4.23)	NR	NR	NR	pCASL	3	WB	resting-state rCBF	NS	0.87
CHR	*Allen et al., 2018* ○ [48]	UHR	77	44/33	22.6 (3.6)	NR	NR	NR	pCASL	3	ROI	resting-state rCBF	UHR > HC (2)	0.83
	Allen et al., 2016 ○ [49]	UHR	52	23/29	22.4 (4.4)	NR	NR	NR	pCASL	3	WB	resting-state rCBF	UHR > HC (8)	0.83
Dynamic susceptibility contrast														
	Talati et al., 2015 [126]	SZ, SZA	15	10/5	36.2 (12.6)	61.1 (13.3)	352.50 (160.4)	10.5 (8.8)	DSC	3	ROI	resting-state rCBF	NS	0.80
SSD	*Bellani et al., 2011* x [108]	SZ	47	31/16	37.0 (11.4)	NR	249.0 (NR)	12.0 (NR)	DSC	1.5	ROI	resting-state rCBF	NS	0.73
	Peruzzo et al., 2011 x [120]	SZ	39	25/14	37.1 (11.5)	NR	245.9 (170.6)	12.3 (10.2)	DSC	1.5	ROI	resting-state rCBF	NS	0.73
FEP	Squarcina et al., 2015 [44]	FEP	35	16/19	36.2 (8.4)	NR	NR	0.2 (0.3)	DSC	NR	WB	resting-state global CBF	NS	0.60
Blood-oxygen level dependent														
SSD	Friedman et al., 2008 [41]	SZ; smoker +/-	12	10/2	41.5 (8.7)	NR	NR	18.5 (10.2)	BOLD	1.5	WB	Breath hold, cognitive task CVR (MTP, MTT, activation volume, signal change)	SSD > HC (1)	0.71

Table 2. Study characteristics, as well as the quality scores for each study.

Note: Studies are written in bold when included in the meta-analysis. Studies are in italics and marked with a matching symbol when samples are overlapping.

Abbreviations: AVH = auditory verbal hallucinations; ASL = arterial spin labelling; CASL: continuous ASL; CHR = clinical high-risk; CVR = cerebrovascular reactivity; CPZeq = Chlorpromazine equivalent; HC = healthy controls; HR = high-risk; F = female; FEP = first episode psychosis; FES = first episode schizophrenia; M = male; MTT = mean transit time; N: sample size; NVC = neuro-vascular coupling; pASL = pulse ASL; pCASL = pseudocontinuous ASL; NR = not reported; NS = not significant; rCBF = regional cerebral blood flow; SD = standard deviation; SSD = schizophre schizophrenia; SZA = schizoaffective disorder; TRS = treatment resistant schizophrenia; TTP = time to peak; UHR = ultra high-risk

	MNI coordinate	Mean SDM-Z	P	Mean Number of voxels	Jack-Knife score
Hyperperfusion - SSD > HC					
Blobs of ≥ 72 voxels with all peaks SDM-Z ≥ 3.369					
Left lenticular nucleus, putamen, BA48	-28,6,8	3.37 [3.13, 3.77]	<0.001	72 [44, 161]	9 (69%)
Hypoperfusion - HC > SSD					
Blobs of ≥ 14 voxels with all peaks SDM-Z ≤ -2.772					
Left superior frontal gyrus, medial, BA 9	-2,46,30	-3.02 [-3.25, -2.82]	<0.005	94 [21, 174]	10 (77%)
Left middle frontal gyrus, BA 10	-36,56,0	-3.08 [-3.82, -2.93]	<0.005	84 [30, 330]	10 (77%)
Right middle occipital gyrus, BA 18	32,-94,8	-3.08 [-3.3, -2.98]	<0.005	29 [14, 53]	8 (62%)
Left superior temporal gyrus, BA 42	-58,-36,16	-2.78 [-2.85, -2.72]	<0.005	26 [16, 35]	2 (15%)
Left middle occipital gyrus, BA 19	-34,-80,32	-2.89 [-2.91, -2.88]	<0.005	22 [15, 28]	2 (15%)
Right superior occipital gyrus	24,-94,12	-3.52 N/A	<0.001	139 N/A	1 (8%)
Left supramarginal gyrus	-58,-36,24	-2.77 N/A	0.003	14 N/A	1 (8%)
Left anterior cingulate / paracingulate gyri	2,46,14	-3.08 N/A	0.001	145 N/A	1 (8%)

Table 3. Brain regions of significant difference in regional cerebral blood flow (rCBF) between patients with SSD and healthy controls.

Note: Jack-knife analysis was scored out of 13 studies. Voxel threshold: uncorrected, p<0.005; TFCE corrected for FWE p<0.025. Peak height threshold: peak SDM-Z > |1.0|. Extent threshold: cluster size ≥ 10 voxels.

Abbreviations: FWE = familly-wise error; HC = healthy controls; MNI = Montreal Neurological institute; SDM-Z = seed based d mapping z score; SSD = schizophrenia spectrum disorders; TFCE = threshold-free cluster enhancement.

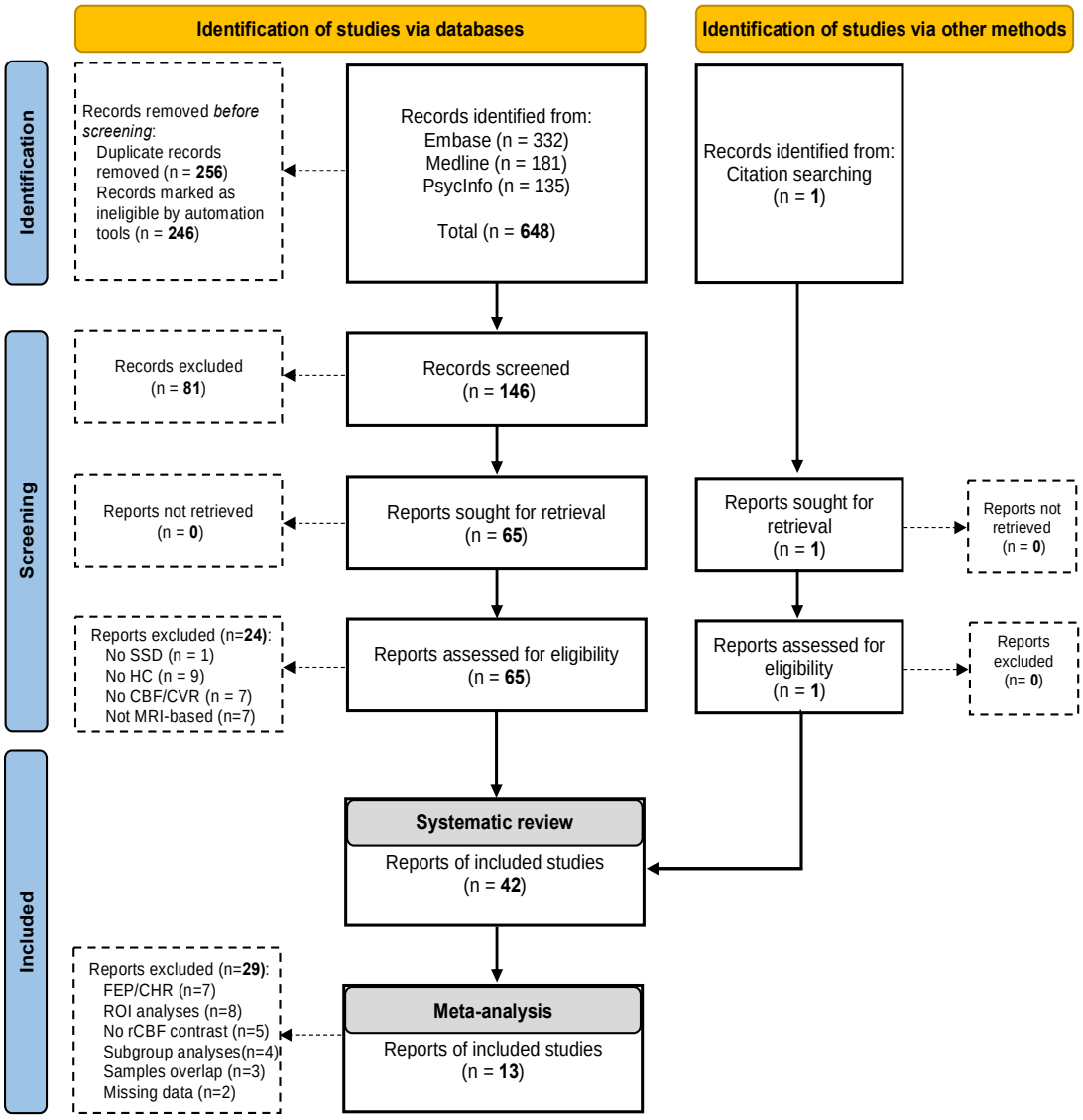

Figure 1. Flow chart of the litterature search

Abbreviations: CBF = cerebral blood flow; CVR = cerebrovascular reactivity; HC = healthy controls; SSD = schizophrenia spectrum disorders.

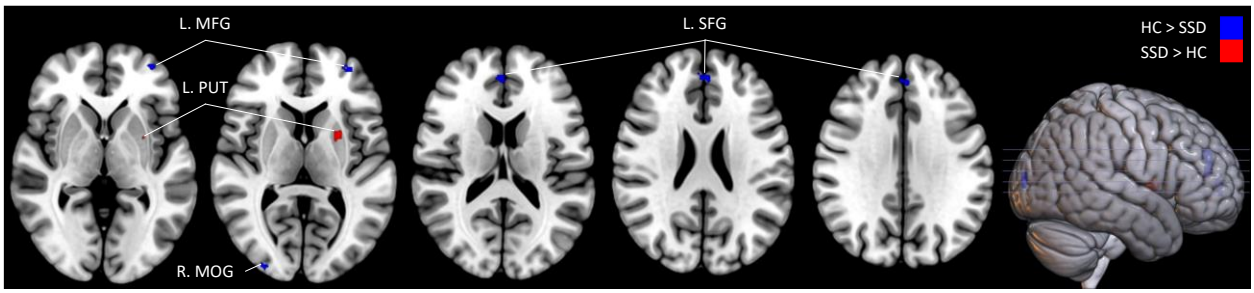

Figure 2. Illustration of significant clusters of regional cerebral blood flow (rCBF) difference between patients with schizophrenia-spectrum disorders (SSD) and healthy controls with uncorrected threshold (p<0.005).
Note: Clusters in blue represent decreased rCBF (hypoperfusion) in SSD patients when compared to HC and clusters in red represent increased rCBF (hyperperfusion) in SSD patients when compared to HC. For illustration purpose, the firgure displays results of the meta-analysis including all 13 studies. Results are overlaid with a MRIcron template for illustration (www.mricro.com/mricron).
Abbreviations: HC = healthy controls; *L = left;* MFG = middle frontal gyrus; MOG = middle occipital gyrus; PUT = putamen; R = right; SFG = superior frontal gyrus; SSD = schizophrenia-spectrum disorders.

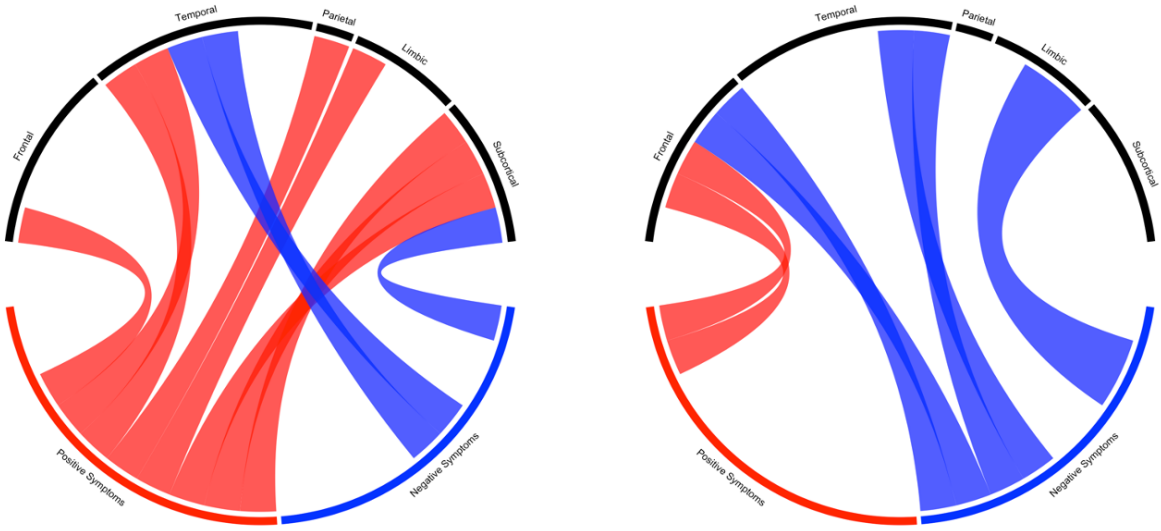

Figure 3. Significant A) positive and B) negative correlations between rCBF and positive or negative symptoms.
Note: the size of the link is reflective of the number of studies repporting the same association.
Abbreviations: ACC = anterio cingulate cortex; ANG = angular cortex; HIP = hippocampus; IFG = inferior frontal gyrus; INS = insula; ITG = inferior temporal gyrus; MTG = middle frontal gyrus; MTG = middle temporal gyrus; PAL = pallidum; PreCG = precentral gyrus; PUT = putamen; SFG = superior frontal gyrus; SPG = superior parietal gyrus; STR = striatum.